Inorganic Chemistry

Article

pubs.acs.org/IC

Assembly of Heterometallic Rigid-Rod Complexes and Coordination Oligomers from Gold(I) Metalloligands

Verónica Cámara,[†] Natalia Barquero,[†] Delia Bautista,[‡] Juan Gil-Rubio,*[,†] and José Vicente*[,†]

[†]Grupo de Química Organometálica, Departamento de Química Inorgánica, Facultad de Química, and [‡]SAI, Universidad de Murcia, E−30071 Murcia, Spain

S *Supporting Information*

ABSTRACT: The reactions of $TpylC_6H_4C\equiv CAuL$ (Tpyl = 2,2′:6′,2″-terpyridin-4′-yl; L = PPh_3, CNXy; Xy = 2,6-dimethylphenyl) with $MX_2\cdot nH_2O$ (M = Fe, X = ClO_4; M = Co, X = BF_4; M = Zn, X = TfO, ClO_4) in a 2:1 molar ratio give complexes $[M(TpylC_6H_4C\equiv CAuL)_2]X_2$. Similarly, the reactions of PPN$[(TpylC_6H_4C\equiv C)_2Au]$ (PPN = $(Ph_3P)_2N$) with an equimolar amount of $MX_2\cdot nH_2O$ give coordination oligomers $[M\{(TpylC_6H_4C\equiv C)_2Au\}]_nX_n$ (M = Fe, Zn, X = ClO_4; M = Co, X = BF_4). The complexes and oligomers have been isolated and characterized. The crystal structures of $[Fe(TpylC_6H_4C\equiv CAuCNXy)_2](ClO_4)_2$ and $[Co(TpylC_6H_4C\equiv CAuPPh_3)_2](BF_4)_2$ have been determined by X-ray diffraction. The hydrodynamic sizes of complexes $[M(TpylC_6H_4C\equiv CAuPPh_3)_2]X_2$ and coordination oligomers $[M\{(TpylC_6H_4C\equiv C)_2Au\}]_nX_n$ have been studied by NMR diffusion spectroscopy and dynamic light scattering measurements.

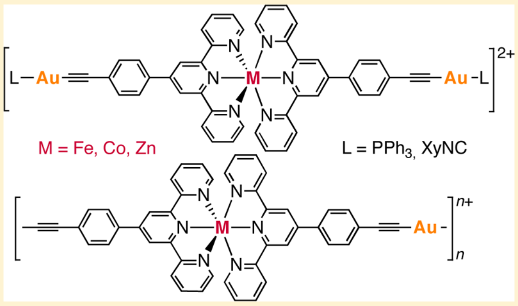

INTRODUCTION

Transition-metal complexes containing the 2,2′:6′,2″-terpyridine ligand have been intensively used in supramolecular chemistry[1−5] because of their large association constants,[6,7] reversible nature,[6−8] and singular redox and photophysical properties.[9−13] Among the terpyridyl-functionalized building blocks reported, those substituted at the 4′-position (Tpyl = 2,2′:6′,2″-terpyridin-4′-yl, Chart 1) are of special interest because the resulting pseudooctahedral $M(Tpyl)_2^{n+}$ complexes can act as linear linkers with a well-defined stereochemistry. For these reasons, Tpyl-containing ligands have been successfully employed in the programmed self-assembly of electro- or photoactive polynuclear complexes by reaction with transition-metal cations.[1−5] On the basis of these reactions, a remarkable variety of supramolecular structures are accessible, such as donor−acceptor heteronuclear complexes,[10,12,14] macrocycles,[15−17] nanopolyhedra,[18,19] molecular racks and grids,[13,20] metallodendritic structures,[3,21−24] and coordination polymers.[3,5,7,25−27]

Chart 1. Reported Alkynyl Au(I) Metalloligands Containing Terpyridyl Units

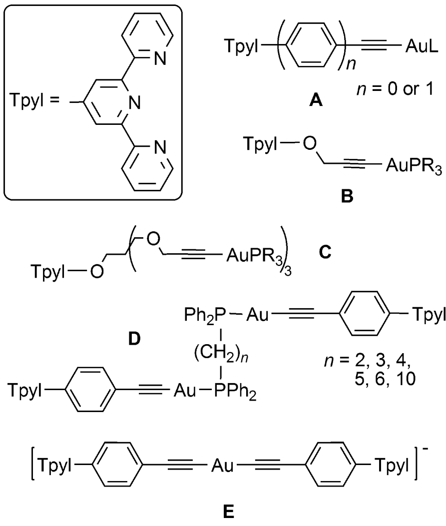

Special attention has been directed to the preparation of rod-like coordination polymers by reaction of rigid ligands containing two oppositely disposed Tpyl groups with an equimolar amount of a metal cation.[7,25−28] These polymers present unusual physical properties which arise from the presence of $M(Tpyl)_2^{n+}$ units in their conjugated backbone. In addition, owing to the reversibility of the M-Tpyl interaction, they have a dynamic nature that can be exploited for the generation of self-healing or stimuli-sensitive materials.[5,7,26,27,29−45]

The supramolecular chemistry of Au(I) alkynyl complexes has attracted increasing interest,[46] motivated mainly by the phenomenon of aurophilicity[47,48] and their remarkable luminescent properties.[49−52] Thus, Au(I) alkynyls have been used as building blocks for the assembly of supramolecular structures such as coordination polymers,[53] metallomacrocycles,[54] catenanes,[54] bioorganometallic complexes,[55−57] nanosheets,[58] and luminescent gels.[59] We have recently reported the

Received: January 23, 2015
Published: June 18, 2015

DOI: 10.1021/acs.inorgchem.5b00176

self-assembly of Au(I) metalloligands containing 2,2′-bipyridyl donors and metal cations to produce polyheteronuclear complexes with unprecedented triple helical structures. The success of this supramolecular event comes from a subtle interplay between aurophilic contacts, π−π interactions, and solvophobic effects.[60−62] Moreover, the presence of an ethynylene spacer connecting the Au atom to the donor group is a key element because (a) Au-alkynyl complexes are stable and easily available, (b) the rigid linear AuC≡C moiety allows a better control over the supramolecular structure than a flexible linker, and (c) they present a low sterical hindrance toward the mutual approach of the Au centers, which is a requisite for the existence of aurophilic interactions. As a continuation of these studies, we directed our attention to the coordination of Au(I) alkynyl metalloligands functionalized with Tpyl donors to metal cations because these reactions could afford heteronuclear complexes and coordination polymers with new structural motifs and interesting photophysical properties.

The groups of Constable, Chen, and us have reported several alkynyl Au(I) metalloligands containing Tpyl groups with different structural designs (Chart 1).[63−66] These include complexes containing one Tpyl group linked to one (**A** and **B**) or three Au centers (**C**),[63−65] neutral flexible digold complexes bearing two Tpyl units (**D**),[63,65,66] and an anionic rigid monogold complex containing two Tpyl units (**E**).[63] Surprisingly, despite the stability and easy availability of these metalloligands, their coordinative behavior is still unexplored, except for the spectrophotometric titration of some metalloligands of the type **D** with lanthanide diketonates, where the structures of the formed complexes were not elucidated.[66]

Herein we report the assembly of heteronuclear complexes and coordination oligomers by reaction of Au(I) metalloligands of the types **A** and **E** with metal cations. The resulting nanometer-sized rod-like complexes and oligomers have been isolated, and their structures have been properly characterized using X-ray crystallography, NMR diffusion studies, and dynamic light scattering (DLS) measurements.

■ RESULTS AND DISCUSSION

Synthesis and Characterization of Au(I)/M(II) Complexes and Coordination Oligomers. The reaction of $TpylC_6H_4C{\equiv}CAuL$ (L = PPh_3, CNXy; Xy = 2,6-dimethylphenyl) with hydrated Fe(II), Co(II), or Zn(II) salts in a 2:1 molar ratio affords complexes $[M(TpylC_6H_4C{\equiv}CAuL)_2]X_2$ in high yield as purple, orange-brown, or pale-yellow solids, respectively (Scheme 1).

Coordination oligomers $[M\{(TpylC_6H_4C{\equiv}C)_2Au\}]_nX_n$ (M = Fe, Zn, X = ClO_4; M = Co, X = BF_4) precipitate by addition of a solution of MX_2 in MeCN to a solution of PPN[$(TpylC_6H_4C{\equiv}C)_2Au$] in CH_2Cl_2 (Scheme 2). They are insoluble in all solvents except in DMSO, where they present a moderate solubility.

Scheme 1. Synthesis of the New Heteronuclear Complexes $[M(TpylC_6H_4C{\equiv}CAuL)_2]X_2$

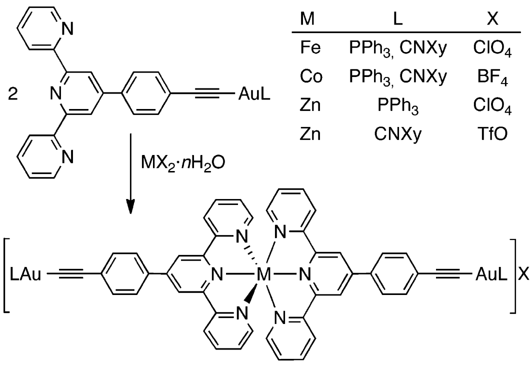

M	L	X
Fe	PPh_3, CNXy	ClO_4
Co	PPh_3, CNXy	BF_4
Zn	PPh_3	ClO_4
Zn	CNXy	TfO

Scheme 2. Synthesis of the Coordination Oligomers $[M\{(TpylC_6H_4C{\equiv}C)_2Au\}]_nX_n$

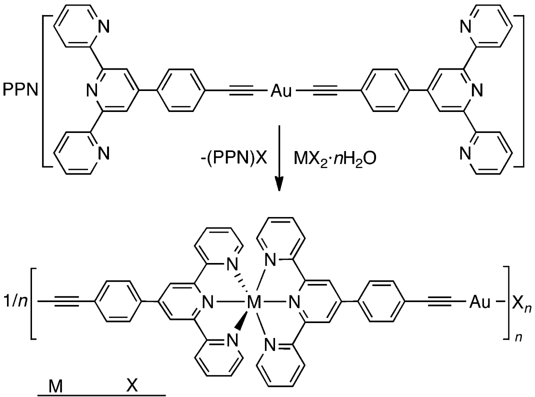

M	X
Fe, Zn	ClO_4
Co	BF_4

$PPN^+ = (Ph_3P)_2N^+$

The positive-ion electrospray ionization mass spectra (ESI-MS) of complexes $[M(TpylC_6H_4C{\equiv}CAuL)_2]X_2$ show always the expected isotopic distributions for $[M(TpylC_6H_4C{\equiv}CAuL)_2]^{2+}$ cations in a high relative abundance, whereas monopositive aggregates between a cation and an anion are observed in all cases except for complexes containing the CNXy ligand. In contrast, the positive-ion ESI-MS of the coordination oligomers $[M\{(TpylC_6H_4C{\equiv}C)_2Au\}]_nX_n$ show the isotopic distribution for cationic fragments resulting from decoordination of one Tpyl moiety or from protonolysis of a Au−C bond. Fragments with n = 1 or 2 are detected with a high relative abundance in all cases, but longer chain fragments are only detected for M = Fe or Zn with low abundances (see Experimental Section). $[Fe_7(TpylC_6H_4C{\equiv}C)_{14}Au_6H_2]^{8+}$ and $[Zn_4(TpylC_6H_4C{\equiv}C)_9Au_5]^{4+}$ are the largest fragments observed for the Fe(II) and Zn(II) oligomers, respectively.

The IR spectra of all complexes and oligomers show the band corresponding with the ν(C≡C) mode in the range 2087−2122 cm^{-1}. Additionally, the IR spectrum of the isonitrile complexes show a strong band at 2194−2200 cm^{-1} corresponding to the ν(C≡N) mode. The ν(C≡C) and ν(C≡N) bands are not significantly shifted respect to the free metalloligands.[63] The obtained complexes and oligomers show the characteristic bands for the ClO_4^- (1080−1099 and 621−623 cm^{-1}), BF_4^- (1056−1058 cm^{-1}), and TfO^- (1260, 1031, 638 cm^{-1}) anions.

The number of signals in the NMR spectra of the complexes and oligomers is in agreement with their symmetry. Thus, as expected for pseudooctahedral complexes containing two mutually perpendicular terpyridine ligands, the ^1H NMR spectra show seven signals corresponding with the terpyridine and C_6H_4 protons. These resonances appear at similar δ values in all the complexes and oligomers containing the same M(II) cation (Figure 1). In the coordination oligomers the signals are broader than in the complexes (Figure 1), and no signals assignable to the terminal groups of the oligomers are detected, probably because of their low intensity and the broadness of the spectra. Additionally, no signals for the PPN^+ cation are

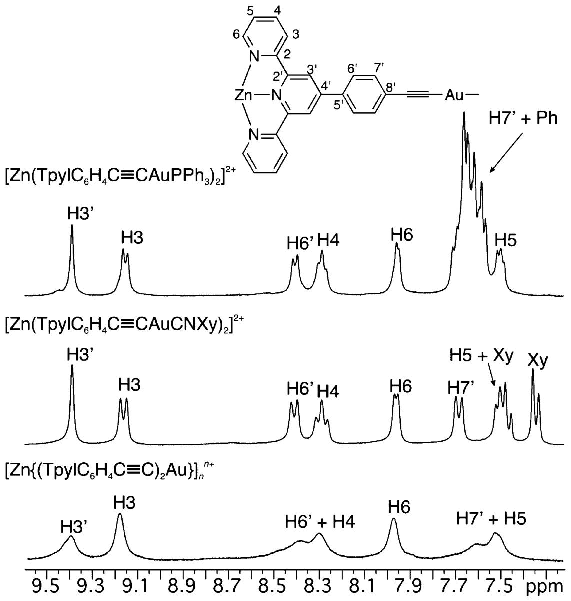

Figure 1. ^{1}H NMR spectra of the complexes $[Zn(TpylC_6H_4C\equiv CAuL)_2]^{2+}$ (L = PPh_3, CNXy) and the oligomer $[Zn\{(TpylC_6H_4C\equiv C)_2Au\}]_n^{n+}$ in DMSO-d_6.

observed, which, together with the characteristic ClO_4^- or BF_4^- anion bands observed in the IR spectra, indicate that the oligomers present a positive net charge.

The NMR spectra of Co(II) heterometallic complexes are severely affected by the paramagnetism of this metal ion, giving rise to broad ^{1}H resonances that appear along a large chemical shift range (91.8–4.9 ppm). The ^{1}H and ^{13}C spectra were assigned with the help of 2D-correlation experiments and by comparing the observed chemical shifts with those reported for Co(II) bis(terpyridine) complexes.[67−69] In addition, complex $[Co(TpylC_6H_4C\equiv CH)_2](BF_4)_2$ was prepared to confirm the assignments (see Supporting Information). The proton shifts depend on the position of the protons respect to the Co(II) atom. Thus, the pyridinic H6, H3, H3′, and H5 protons are the most paramagnetically shifted (δ = 91.94–40.84 ppm), which is in agreement with their shorter distances to the Co atom. In contrast, H4 and the C_6H_4 protons appear deshielded by less than 4 ppm with respect to their diamagnetic Zn(II) or Fe(II) analogues, and the C≡CH, Xy, and PPh_3 protons resonate in the usual ranges for diamagnetic complexes.

The complexes containing the $TpylC_6H_4C\equiv CAuPPh_3$ metalloligand show a singlet at 42.2 (Fe), 44.4 (Co), and 42.6 (Zn) ppm in their $^{31}P\{^1H\}$ NMR spectra. These δ values are similar to those observed for the free metalloligand (42.8 ppm).[63]

The C, H, and N contents of the coordination oligomers determined by combustion analyses agree with a general composition of the type $[M\{(TpylC_6H_4C\equiv C)_2Au\}]_nX_n\cdot MX_2\cdot(H_2O)_x$, where the calculated n values are 4.3 (M = Fe, Zn; X = ClO_4) and 8.8 (M = Co; X = BF_4). This could be attributed to (a) the coprecipitation of water during oligomer precipitation, and (b) the coordination of $MX_2(H_2O)_x$ units to the Tpyl groups of both ends of the oligomer chains.

Crystal Structures. The crystal structures of $[Fe(TpylC_6H_4C\equiv CAuCNXy)_2](ClO_4)_2\cdot(MeCN)_2$ (Figure 2) and $[Co(TpylC_6H_4C\equiv CAuPPh_3)_2](BF_4)_2\cdot(MeCN)_4$ (Figures 3 and 4) were determined by single-crystal X-ray diffraction. In both complexes, two metalloligands are coordinated to the metal cations in a distorted octahedral geometry. Thus, the M–N_{axial} bonds are ca. 0.1 Å shorter than the M–$N_{equatorial}$ bonds, and the N_{axial}–M–$N_{equatorial}$ angles corresponding to the same Tpyl unit are smaller than 90° (79.5–80.7°), whereas those between different Tpyl units are larger than 90° (100.6–98.2°). Additionally, although the N_{axial}–M–N_{axial} angle is close to 180°, the $N_{equatorial}$–M–$N_{equatorial}$ angles between nitrogen atoms mutually in *trans* are considerably smaller than 180° (159.2–162.3°). These distances and angles agree with those observed in other terpyridine complexes of Fe(II)[70−72] and Co(II),[73,74] and could be attributed to the steric constraints imposed by the rigidity of these ligands, together with Jahn–Teller effects.

The Au–$C_{alkynyl}$, Au–P, Au–$C_{isocyanide}$, and C≡C bond distances are similar to those observed in the free metalloligand[63] or in $[Au(C\equiv CAr)(CNXy)]$ (Ar = Ph, $C_6H_4NO_2$-

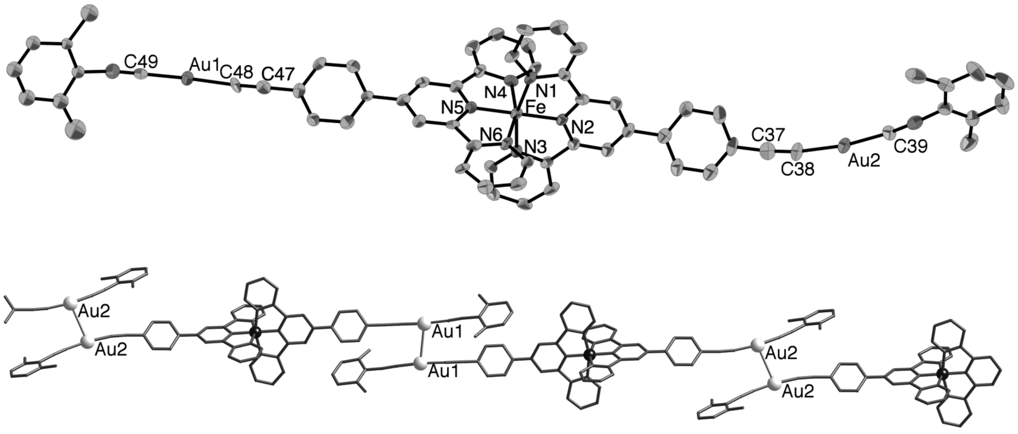

Figure 2. Top: Molecular structure of the cations in the crystal structure of the salt $[Fe(TpylC_6H_4C\equiv CAuCNXy)_2](ClO_4)_2\cdot(MeCN)_2$ (50% thermal ellipsoids; hydrogen atoms have been omitted for clarity). Bottom: Aurophilic interactions between the $[Fe(TpylC_6H_4C\equiv CAuCNXy)_2]^{2+}$ cations. Selected bond lengths (Å) and angles (deg): Fe(1)–N(1) 1.971(7), Fe(1)–N(2) 1.883(6), Fe(1)–N(3) 1.970(7), Fe(1)–N(4) 1.981(7), Fe(1)–N(5) 1.874(6), Fe(1)–N(6) 1.969(7), Au(1)–C(48) 2.000(8), Au(1)–C(49) 1.929(9), Au(2)–C(38) 1.972(9), Au(2)–C(39) 1.935(8), C(37)–C(38) 1.218(12), C(47)–C(48) 1.144(11), Au(1)····Au(1) 3.327, Au(2)···Au(2) 3.434; C(48)–Au(1)–C(49) 172.6(4), C(47)–C(48)–Au(1) 173.5(8), C(38)–Au(2)–C(39) 171.5(4), C(37)–C(38)–Au(2) 171.7(9).

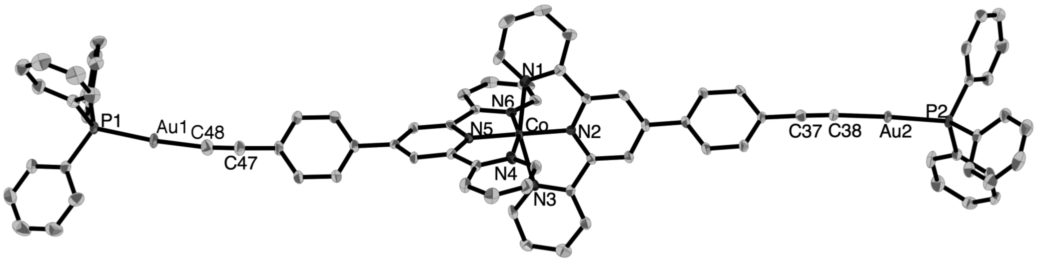

Figure 3. Molecular structure of the cation in the crystal structure of the salt $[Co(TpylC_6H_4C{\equiv}CAuPPh_3)_2](BF_4)_2{\cdot}(MeCN)_4$ (50% thermal ellipsoids; hydrogen atoms have been omitted for clarity). Selected bond lengths (Å) and angles (deg): Co(1)−N(1) 2.112(4), Co(1)−N(2) 1.907(4), Co(1)−N(3) 2.118(4), Co(1)−N(4) 2.012(4), Co(1)−N(5) 1.864(4), Co(1)−N(6) 2.009(4), Au(1)−C(48) 1.992(5), Au(1)−P(1) 2.2693(12), Au(2)−C(38) 1.995(4), Au(2)−P(2) 2.2861(12), C(37)−C(38) 1.207(6), C(47)−C(48) 1.192(7); C(48)−Au(1)−P(1) 173.86(15), C(47)−C(48)−Au(1) 172.9(5), C(38)−Au(2)−P(2), 173.91(13), C(37)−C(38)−Au(2) 174.1(4).

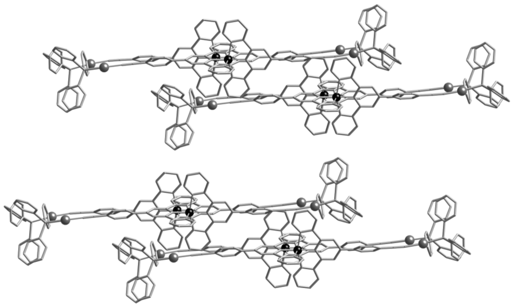

Figure 4. Double layers of cations in the crystal structure of $[Co(TpylC_6H_4C{\equiv}CAuPPh_3)_2](BF_4)_2{\cdot}(MeCN)_4$.

4).[75,76] The C−Au−C≡C and the P−Au−C≡C angles are slightly distorted from linearity.

Short Au···Au intermolecular contacts were found in the structure of $[Fe(TpylC_6H_4C{\equiv}CAuCNXy)_2](ClO_4)_2{\cdot}(MeCN)_2$, which give rise to the formation of parallel chains (Figure 2). In contrast, the crystal structure of $[Co(TpylC_6H_4C{\equiv}CAuPPh_3)_2](BF_4)_2{\cdot}(MeCN)_4$ does not present aurophilic contacts, likely because the bulkier PPh_3 ligands impede the mutual approach of the Au centers. The cationic complexes are packed in a parallel disposition forming double layers (Figure 4), where the bulky $Co(Tpyl)_2$ groups of one sublayer fit with the Au−C≡C moieties of the molecules of the other sublayer. The space between layers is occupied by the BF_4^- ions and MeCN molecules. Weak C−H···F−B bonds are observed between the cation or the solvent molecules and the anions (see Supporting Information).

NMR Diffusion Studies. The measurement of the translational diffusion coefficient (D) by pulsed field-gradient NMR spectroscopy allows determination of the hydrodynamic dimensions of supramolecular species in solution.[77,78] This technique has been used in a qualitative way to probe the formation of supramolecular polymers by reaction of bis(terpyridine) organic ligands with M^{2+} cations.[29,38,39] In these experiments, a marked decrease in D was qualitatively correlated with the formation of slower-diffusing coordination polymers, but the average sizes of these polymers were not determined from the measured diffusion coefficients.

We attempted to quantitatively derive the average hydrodynamic dimensions of the coordination oligomers $[M\{(TpylC_6H_4C{\equiv}C)_2Au\}]_n^{n+}$ from their D values obtained by NMR diffusion experiments. Since these molecules have a rod shape, they were modeled as cylindrical particles of diameter d and length L. With this assumption, the values of d and L can be related to the diffusion coefficient by eq 1.[79−85]

$$D = \frac{K_B T}{3\pi\eta}\frac{\ln P + \gamma}{L} \qquad (1)$$

In this equation P is the ratio L/d, and γ is the end-effect term, which was semiempirically determined by García de la Torre and co-workers:[79]

$$\gamma = 0.312 + (0.565/P) + (0.100/P^2) \qquad (2)$$

To test the suitability of the cylindrical-particle model to the prepared coordination oligomers, we first applied it to complexes $[M(TpylC_6H_4C{\equiv}CAuPPh_3)_2]^{2+}$ (M = Fe, Co, Zn) because they present a well-defined structure in solution, and the crystal structure of one of them has been determined by X-ray diffraction (see below). Their D values (Table 1) fall in a narrow range, which suggests that the dimensions of the three complexes are similar. This is not surprising if we consider that the main structural differences between the three complexes should appear in the central $M(Tpyl)_2$ unit, and the M−N bond distances observed in the crystal structures of $[Fe(TpylC_6H_4C{\equiv}CAuCNXy)_2](ClO_4)_2$, $[Co(TpylC_6H_4C{\equiv}CAuPPh_3)_2](BF_4)_2$, and the related complex $[Zn(TpylC_6H_5)_2](ClO_4)_2$[86] differ by less than 0.25 Å.

Table 1. Diffusion Coefficients (D), Molecular Cylinder Diameter (d) and Length (L) for the Prepared Trinuclear Complexes and Coordination Oligomers

complex	D (10^{-11} m^2 s^{-1})[a]	d (Å)[b]	L (Å)[c]
$[Fe(TpylC_6H_4C{\equiv}CAuPPh_3)_2]^{2+}$	9.18	11.06	39.0
$[Co(TpylC_6H_4C{\equiv}CAuPPh_3)_2]^{2+}$	9.14	11.16	38.4
$[Zn(TpylC_6H_4C{\equiv}CAuPPh_3)_2]^{2+}$	9.21	11.15	38.6
$[Fe\{(TpylC_6H_4C{\equiv}C)_2Au\}]_n^{n+}$	3.12	11.06	224
$[Zn\{(TpylC_6H_4C{\equiv}C)_2Au\}]_n^{n+}$	3.10	11.15	219

[a] Measured in DMSO-d_6 solution ($c = 4.9 \times 10^{-3}$ to 5.3×10^{-3} M at 294−295 K). [b] Determined from the crystal structures (see Results and Discussion). [c] Calculated from the D and d values using eq 1.

For complexes $[M(TpylC_6H_4C{\equiv}CAuPPh_3)_2]^{2+}$, we defined the diameter of the cylindrical model (d) as the average of the two distances between the most external hydrogen atoms of each terpyridine ligand (H4 and H4″ in Figure 5). These distances were directly taken from the crystal structures of $[Co(TpylC_6H_4C{\equiv}CAuPPh_3)_2](BF_4)_2$, $[Fe(TpylC_6H_4C{\equiv}CAuCNXy)_2](ClO_4)_2$ and $[Zn(TpylC_6H_5)_2](ClO_4)_2$.[86] Using these diameters, the experimental D values, and eq 1, we deduced L values in the range 38.4−39.0 Å (Table 1). These values are in reasonable agreement with the metrics observed in the crystal structure of the Co complex (Figure 5), where the

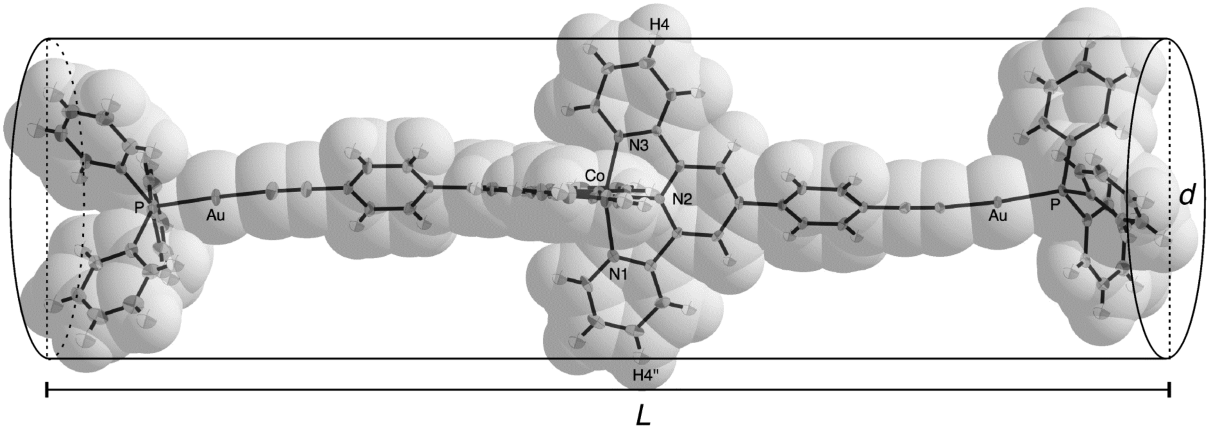

Figure 5. Comparison of the structure of complex $[Co(TpylC_6H_4C{\equiv}CAuPPh_3)_2]^{2+}$ with a cylindrical model of approximate dimensions d = 11 Å and L = 38.5 Å. The atoms are represented as spheres of van der Waals radii.

distance between the centroids of the three *para* hydrogens of each PPh_3 ligand is 35.5 Å, and the distances between the most external couples of phenylic hydrogens are in the range 34.4−38.7 Å (see also the Supporting Information).

Having tested the suitability of the model to estimate the hydrodynamic dimensions of the complexes, we applied it to coordination oligomers $[M\{(TpylC_6H_4C{\equiv}C)_2Au\}]_n^{n+}$. As expected for its bigger size, their diffusion coefficients were considerably smaller than those of the trinuclear complexes (Table 1). Thus, using the measured D values, and considering the oligomers as cylindrical particles with the same diameter (d) than the corresponding trinuclear complexes, L values of 224 and 219 Å were calculated for the Fe and Zn oligomers, respectively (Table 1). To determine the average oligomerization degree, we estimated the length of a monomeric unit in the Fe oligomer as the intramolecular Au−Au distance in the crystal structure of $[Fe(TpylC_6H_4C{\equiv}CAuCNXy)_2](ClO_4)_2$ (27.0 Å). Then, dividing the determined oligomer's length by the estimated length of the monomeric unit, an average oligomerization degree (n) of 8.3 was obtained. The same calculation for the Zn oligomer, using a value of 27.4 Å for the length of the monomeric unit,[87] gave an average n value of 8.0. Since these values were measured in DMSO solution under equilibrium conditions, they are higher than the average n values deduced from the elemental analyses of the precipitated Fe and Zn oligomers (see above), which precipitated in a CH_2Cl_2/MeCN mixture.[26] As a consequence of the low solubility and the paramagnetic effect, we were not able to perform a similar study for the Co(II) oligomer.

DLS and SEC Measurements. DLS measurements[29,88−91] have proved useful in the determination of the size distribution of coordination polymers with a rigid backbone.[29,89−91] Thus, we applied this technique to gain more information on the molecular sizes of oligomers $[M\{(TpylC_6H_4C{\equiv}C)_2Au\}]_nX_n$ and complexes $[M(TpylC_6H_4C{\equiv}CAuPPh_3)_2]X_2$. The measurements were carried out in the conditions used for the NMR diffusion studies. The plots of the scattered intensity against the particle hydrodynamic diameter of the Co and Zn oligomers (Figure 6, top) show monomodal distributions which range in the intervals 40−300 nm, and 10−150 nm, respectively. These particle size values should be interpreted with caution because the software assumes a spherical particle shape for the determination of the size distributions. In addition, the amount of small-size molecules can be underestimated in the intensity size distributions because larger particles scatter a higher amount of light intensity than smaller ones.[88,92] Hence, to assess the presence of short oligomers, the number size distributions were calculated using the Mie theory (Figure 6, bottom). No peaks at small diameters were observed in the number size distribution for the Co oligomer, and only a very small peak at ca. 1.5 nm was observed for the Zn oligomer. Thus, although the determined hydrodynamic diameters cannot be directly compared with the hydrodynamic dimensions determined by NMR assuming a cylindrical molecular shape, the DLS results suggest that compounds $[M\{(TpylC_6H_4C{\equiv}C)_2Au\}]_nX_n$ are mainly formed by mixtures of oligomers with hydrodynamic diameters on the order of tens of nanometers and a broad distribution of chain lengths.

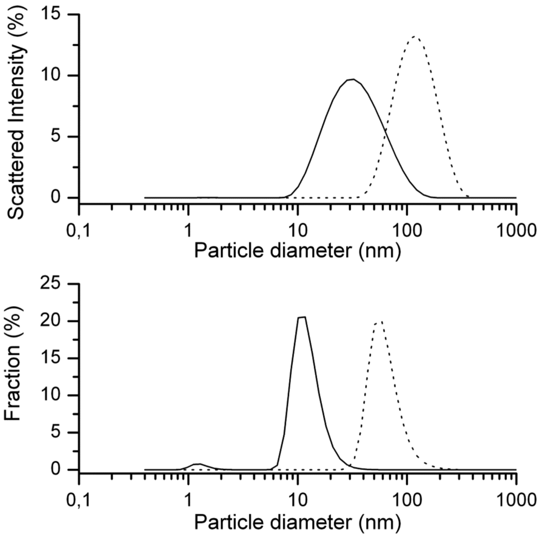

Figure 6. Distributions of the scattering intensity (top) or the fraction of particles (bottom) with the hydrodynamic diameter. Determined by DLS on 5 mM DMSO solutions of compounds $[Co\{(TpylC_6H_4C{\equiv}C)_2Au\}]_n(BF_4)_n$ (dotted line) and $[Zn\{(TpylC_6H_4C{\equiv}C)_2Au\}]_n(ClO_4)_n$ (solid line).

The intensity size distributions of complexes $[M(TpylC_6H_4C{\equiv}CAuPPh_3)_2]X_2$ (M = Co, X = BF_4; M = Zn, X = ClO_4) are bimodal (Figure 7, top). They show a narrow peak whose maximum intensity corresponds with a hydrodynamic diameter around 1.5 nm, which is of the same order of magnitude as the molecular dimensions determined by NMR diffusion measurements, and a broad peak corresponding to larger particles.

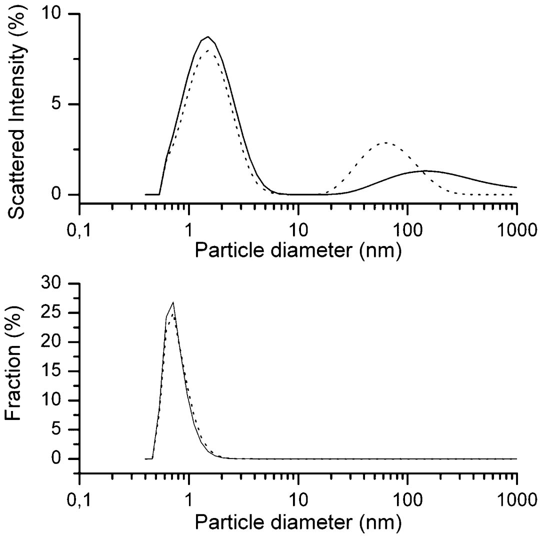

Figure 7. Distribution of the scattering intensity (top) or the fraction of particles (bottom) with the hydrodynamic diameter. Determined by DLS on 5 mM DMSO solutions of compounds $[Co(TpylC_6H_4C{\equiv}CAuPPh_3)_2](BF_4)_2$ (dotted line) and $[Zn(TpylC_6H_4C{\equiv}CAuPPh_3)_2](ClO_4)_2$ (solid line). In the intensity distributions, the ratios of the areas of the peaks corresponding to the large and small particles are 0.4 (Co complex) and 0.3 (Zn complex).

However, considering the smaller areas of the broad peaks, and the effect of the particle size on the scattered intensity (see above), these large particles should represent a very small fraction of the total weight of the solute.[89,93] In fact, they are neither detected in the number particle size distributions (Figure 7, bottom) nor in the NMR spectra of the measured samples (Supporting Information). The size distribution of both Fe complex and oligomers could not be determined because they scattered very poorly in these conditions.

We attempted to assess the size distribution of the oligomers by size exclusion chromatography (SEC). However, as has been previously noted by several authors,[3,7,27,38] the SEC analysis of coordination polymers containing labile bis(terpyridine) metal units in their main chain is hindered by (i) the reversible nature of their association equilibrium, which is sensitive to the concentration changes that occur inside the chromatographic column, and (ii) the adsorption of the charged molecules on the stationary phase. In addition, appropriate standards for the determination a meaningful size distribution of these rigid-rod molecules are not available. In our case, the SEC traces of the Fe, Co, and Zn oligomers, measured in dimethylformamide, showed narrow peaks at relatively short retention times, which are indicative of high molecular weight chains, together with broad peaks which decay very slowly (Supporting Information). These features are likely produced by chain dissociation and adsorption on the stationary phase, and impeded the determination of the molecular weight distribution of the samples.

CONCLUSIONS

The assembly of heterometallic complexes by using terpyridine-functionalized Au(I) metalloligands has been studied for the first time. Trinuclear complexes $[M(TpylC_6H_4C{\equiv}CAuL)_2]X_2$ (M = Fe, Co, Zn) have been isolated and structurally characterized. Multicharged coordination oligomers $[M\{(TpylC_6H_4C{\equiv}C)_2Au\}]_nX_n$, containing alternated $Au(C{\equiv}C)_2^-$ and $M(Tpyl)_2^{2+}$ units in their chains have been isolated and characterized. These complexes and oligomers present rigid-rod structures whose hydrodynamic dimensions in DMSO were studied by means of diffusion NMR spectroscopy and DLS measurements. A reasonably good agreement was found between (i) the hydrodynamic dimensions of the trinuclear complexes, determined by diffusion NMR spectroscopy using a cylindrical model, (ii) their crystallographic molecular dimensions, and (iii) their hydrodynamic diameters determined by DLS. The coordination oligomers present a broad chain length distribution, as determined by DLS. An average hydrodynamic length of ca. 22 nm was estimated by diffusion NMR spectroscopy for the coordination oligomers using a cylindrical model.

EXPERIMENTAL SECTION

Table 2. Crystallographic Data

	$[Co(TpylC_6H_4C{\equiv}CAuPPh_3)_2](BF_4)_2\cdot(MeCN)_4$	$[Fe(TpylC_6H_4C{\equiv}CAuCNXy)_2](ClO_4)_2\cdot(MeCN)_2$
formula	$C_{90}H_{70}Au_2B_2CoF_8N_{10}P_2$	$C_{68}H_{52}Au_2Cl_2FeN_{10}O_8$
cryst size (mm^3)	0.09 × 0.08 × 0.01	0.18 × 0.08 × 0.08
cryst syst	triclinic	triclinic
space group	$P\bar{1}$	$P\bar{1}$
a (Å)	12.5960(11)	14.5018(13)
b (Å)	17.2820(15)	15.4855(14)
c (Å)	18.9869(16)	15.6214(14)
α (deg)	101.911(3)	67.063(2)
β (deg)	99.445(3)	77.990(2)
γ (deg)	92.717(3)	70.603(2)
V (Å^3)	3975.2(6)	30034.8(5)
Z	2	2
ρ_{calcd} (g cm^{-3})	1.654	1.814
F_{000}	1954	1624
μ (mm^{-1})	4.001	5.214
transmissions	0.9281−0.7805	0.6805−0.4538
θ range (deg)	2.12−28.28	1.49−26.37
reflns collected	205358	32942
R_{int}	0.1035	0.0644
data/restraints/params	19706/49/1034	12330/15/806
GOF	1.058	0.996
R_1[a]	0.0420	0.0543
wR_2[b]	0.0805	0.1295
largest diff peak (e Å^{-3})	1.640 and −1.342	2.444 and −1.321

[a] $R_1 = \Sigma||F_o| - |F_c||/\Sigma|F_o|$ for reflections with $I > 2\sigma(I)$. [b] $wR_2 = [\Sigma[w(F_0^2 - F_c^2)^2]/\Sigma[w(F_0^2)^2]]^{0.5}$ for all reflections; $w^{-1} = \sigma^2(F^2) + (aP)^2 + bP$, where $P = (2F_c^2 + F_0^2)/3$ and a and b are constants set by the program.

General Considerations. Compounds $PPN[(TpylC_6H_4C{\equiv}C)_2Au]$ and $TpylC_6H_4C{\equiv}CZ$ (Z = H, $AuPPh_3$, AuCNXy)[63,94] were prepared according to previously reported methods. Other reagents were obtained from commercial sources and used without further purification. HPLC-grade MeCN (Baker), and analytical-grade Et_2O were used as received. Analytical-grade CH_2Cl_2 was previously distilled over CaH_2. C, H, N, and S analyses were carried out with Carlo Erba 1108 and LECO CHS-932 microanalyzers. The amount of H_2O in the elemental analyses of the complexes was determined by integration of their ^1H NMR spectrum after subtracting the integral of the solvent water to the integral of the water signal of the sample. For the oligomers, a similar determination could not be carried out with accuracy because of their lower solubility and broad spectra. NMR spectra were measured on Bruker Avance 200, 300, 400, and 600 instruments. ^{1}H NMR spectra were referenced according to the following values for the residual protonated solvent signals: $CDHCl_2$ (5.32 ppm), $CHCl_3$ (7.26 ppm), CHD_2CN (1.95 ppm), DMSO-d_5 (2.50 ppm). ^{13}C{^{1}H} spectra were referenced using the following values for the solvent signals: CD_2Cl_2 (53.8 ppm), $CDCl_3$ (77.0 ppm), CD_3CN (1.32 ppm), DMSO-d_6 (39.5 ppm). ^{31}P{^{1}H} spectra were referenced respect to external H_3PO_4 (0 ppm). Abbreviations used: br (broad), s (singlet), d (doublet), t (triplet), m (multiplet), vd (virtual doublet), Tpyl (2,2′:6′,2″-terpiridine-4′-yl). Assignments of ^{1}H and ^{13}C{^{1}H} NMR spectra are based on COSY, HMQC, and HMBC experiments. Figure 1 shows the atom numbering used in NMR assignments. The ESI mass spectra of the complexes were measured on an Agilent 6620 Accurate Mass TOF LC/MS spectrometer. The samples were dissolved in MeCN, and the same solvent was used as carrier, except for complexes $[M(TpylC_6H_4C{\equiv}CAuCNXy)_2](ClO_4)_2$ (M = Fe, Zn), for which the carrier was a solution of $NH_4(HCO_2)$ (5 mM) and HCO_2H (1%) in MeOH/H_2O (75:25). The Co and Zn oligomers were measured on the same mass spectrometer, using DMSO as the solvent and MeCN (Co and Zn oligomers) or MeOH (Zn oligomer) as the carrier. $[Fe\{(TpylC_6H_4C{\equiv}C)_2Au\}]_n(ClO_4)_n$ was measured on a LCQ Deca XPlus spectrometer, using DMSO/acetone as the solvent and MeOH as the carrier. Δ is the deviation of the experimental exact mass respect to the calculated one in ppm. Melting points were determined on a Reichert apparatus in an air atmosphere.

Diffusion experiments were performed on 4.9−5.3 mM solutions of the complexes in DMSO-$d_6$using a Bruker Avance 400 spectrometer equipped with a BBO 5 mm probe. The measurements were carried out without spinning and with the airflow disconnected. The shape of the gradient was sinusoidal, and its strength was linearly increased in 32 steps from 2% to 95% of the maximum level. The standard ledbpgp2s pulse program supplied by Bruker was used (longitudinal eddy-current delay with bipolar gradient pulse pair and 2 spoil gradients).[95] The diffusion coefficients were calculated with the T_1/T_2 processing module of the Bruker Topspin 2.0 software using a one-component exponential fit to eq 3.

$$I = I_0 \exp[-D(\gamma\delta G)^2(\Delta - \delta/3)] \qquad (3)$$

where D = diffusion coefficient, γ = magnetogyric ratio for hydrogen, G = gradient strength, Δ = diffusion time (100 ms), and δ = length of the bipolar diffusion gradient (3.6 ms). In order to test the quality of the data, the signal intensity changes $\ln(I/I_0)$ were plotted against G^2. The plots were linear, which confirmed that the data are suitable for the determination of D using eq 1. The experimental error was estimated as ±5%. The DMSO viscosity values at the temperatures of the measurements were obtained by extrapolation of reported values for different temperatures.[96]

DLS measurements were carried out using a Malvern Zetasizer Nano ZS instrument, equipped with a 4 mW He/Ne laser emitting at 633 nm, a measurement cell, a photomultiplier, and a correlator. The scattering intensity was measured at a 173° angle relative to the source (backscattering). The software calculates the size distribution function, i.e., the hydrodynamic diameter distribution, from the time autocorrelation function of the scattering intensity fluctuations. Each measurement was set to 15 runs of 20 s each. All DLS results are the average of 30 measurements performed during approximately 4 h. The intensity distribution is the primary information about size distribution in DLS measurements. However, the percentage of small particles can be distorted by the high amount of light intensity scattered by particles of big size. Other distributions that better represent the proportions of the different structures can be derived from some assumptions. Thus, the number distribution was calculated from the DLS intensity distribution using the Mie theory, which assumes the spherical shape of the particles, the absence of any error in the intensity distribution, and the exact knowledge of the refractive index of the particle as well as the scattering angle. Therefore, the number distribution derived from DLS is best used for comparison purposes and should never be considered absolute.

Caution! Perchlorate salts of transition-metal complexes are potentially explosive. Only small quantities should be prepared, and the samples should be handled with great care.

Synthesis of $[M(TpylC_6H_4C{\equiv}CAuL)_2]X_2$ (M = Fe, Co, Zn; L= PPh_3, CNXy; X = BF_4, ClO_4, TfO). To a suspension of $TpylC_6H_4C{\equiv}CAuL$ in MeCN (15 mL), $MX_2{\cdot}nH_2O$ was added. The resulting solution was stirred for 2 h at room temperature and concentrated under vacuum ca. 2 mL. Addition of Et_2O (30 mL) precipitated a solid, which was filtered, washed with CH_2Cl_2 (1 × 5 mL) and Et_2O (3 × 5 mL), and dried under a vacuum.

$[Fe(TpylC_6H_4C{\equiv}CAuPPh_3)_2](ClO_4)_2$. Prepared from $TpylC_6H_4C{\equiv}CAuPPh_3$ (98 mg, 0.12 mmol) and $Fe(ClO_4)_2{\cdot}6.4H_2O$ (23 mg, 0.062 mmol). A purple solid was obtained. Yield: 115 mg, 0.061 mmol, 99%. Mp: 260−265 °C. Anal. Calcd for $C_{82}H_{58}Au_2Cl_2FeN_6P_2O_8{\cdot}(H_2O)_2$: C 52.55, H 3.33, N 4.48. Found: C 52.17, H 3.18, N 4.73. IR (KBr) $\tilde{\nu}$ (cm^{-1}): 2107 (C≡C). ^{1}H NMR (300.1 MHz, CD_3CN): δ 9.18 (s, 4H, H3′), 8.62 (d, $^3J_{HH}$ = 8.1 Hz, 4H, H3), 8.27 (vd, J = 8.4 Hz, 4H, H6, C_6H_4), 7.91 (td, $^3J_{HH}$ = 7.8, $^4J_{HH}$ = 1.2 Hz, 4H, H4), 7.80 (vd, J = 8.1 Hz, 4H, H7, C_6H_4), 7.65−7.57 (m, 30H, Ph), 7.20 (d, $^3J_{HH}$ = 4.8 Hz, 4H, H6), 7.08 (t, $^3J_{HH}$ = 6.3 Hz, 4H, H5); (400.9 MHz, DMSO-d_6): δ 9.68 (s, 4H, H3′), 9.07 (d, $^3J_{HH}$ = 8.0 Hz, 4H, H3), 8.53 (vd, J = 8.0 Hz, 4H, H6, C_6H_4), 8.04 (t, $^3J_{HH}$ = 8.0, 4H, H4), 7.75 (vd, J = 8.0 Hz, 4H, H7, C_6H_4), 7.67−7.57 (m, 30H, Ph), 7.28 (d, $^3J_{HH}$ = 4.0 Hz, 4H, H6), 7.18 (t, $^3J_{HH}$ = 6.4 Hz, 4H, H5). ^{13}C{^{1}H} NMR (100.8 MHz, CD_3CN): δ 161.2 (C2′), 159.0 (C2), 154.0 (C6), 150.6 (C8′), 139.7 (C4), 135.5 (C5′), 135.2 (d, $^2J_{PC}$ = 14.0 Hz, *o*-Ph), 134.0 (C7, C_6H_4), 132.9 (s, *p*-Ph), 131.0 (d, $^1J_{PC}$ = 56.0 Hz, *i*-Ph,), 130.5 (d, $^3J_{PC}$ = 11.0 Hz, *m*-Ph), 129.1 (C4′), 128.7 (C6′), 128.3 (C5), 124.8 (C3), 122.2 (C3′). The signals of C≡CAu were not observed. ^{31}P{^{1}H} NMR (121.5 MHz, CD_3CN): δ 42.2 (s), (DMSO-d_6): 42.2 (s). ESI-MS m/z: 1737 $[Fe(TpylC_6H_4C{\equiv}CAuPPh_3)_2(ClO_4)]^+$), 1179 ($[(Ph_3PAuC{\equiv}CC_6H_4Tpyl)Fe(TpylC_6H_4C{\equiv}CH)]^+$), 819 ($[Fe(TpylC_6H_4C{\equiv}CAuPPh_3)_2]^{2+}$), 721 ($[Au(PPh_3)_2]^+$), 459 ($[AuPPh_3]^+$). Exact m/z calcd. for ($[Fe(TpylC_6H_4C{\equiv}CAuPPh_3)_2]^{2+}$): 819.1434; found: 819.1457; Δ = 2.8 ppm.

$[Zn(TpylC_6H_4C{\equiv}CAuPPh_3)_2](ClO_4)_2$. Prepared from $TpylC_6H_4C{\equiv}CAuPPh_3$ (63 mg, 0.080 mmol) and $Zn(ClO_4)_2{\cdot}6H_2O$ (15 mg, 0.040 mmol). A light yellow solid was obtained. Yield: 44 mg, 0.023 mmol, 58%. Mp: 201 °C (d). Anal. Calcd for $C_{82}H_{58}Au_2Cl_2N_6O_8P_2Zn{\cdot}(H_2O)_2$: C 52.29, H 3.32, N 4.46. Found: C 52.14, H 3.00, N 4.59. IR (KBr) $\tilde{\nu}$ (cm^{-1}): 2103 (C≡C), 1099, 623 (ClO_4^-). ^{1}H NMR (400.9 MHz, DMSO-d_6): δ 9.39 (br s, 4H, H3′), 9.16 (d, $^3J_{HH}$ = 7.9 Hz, 4H, H3), 8.41 (vd, J = 8.1 Hz, 4H, H6, C_6H_4), 8.28 (t, $^3J_{HH}$ = 7.8, 4H, H4), 7.95 (d, $^3J_{HH}$ = 4.5 Hz, 4H, H6), 7.71−7.57 (m, 34H, Ph and H7, C_6H_4), 7.50 (t, $^3J_{HH}$ = 5.8 Hz, 4H, H5). ^{13}C{^{1}H} NMR (100.8 MHz, DMSO-d_6): δ 154.3 (C8′ or C4′), 149.5 (C2 or C2′), 147.8 (C6), 147.7 (C2′ or C2), 141.3 (C4), 139.8 (C4′ or C8′), 133.9 (d, $^3J_{PC}$ = 13.8 Hz, *o*-Ph), 133.4 (C5′), 132.3 (s, C7′), 132.1 (d, $^4J_{PC}$ = 1.6 Hz, *p*-Ph), 129.7 (d, $^3J_{PC}$ = 11.3 Hz, *m*-Ph), 129.2 (d, $^4J_{PC}$ = 56.0 Hz, *i*-Ph), 128.2 (C6′), 127.7 (C5), 123.5 (C3), 120.7 (C3′), 102.7 (d, $^3J_{PC}$ = 27.6 Hz, C≡CAu). The signal of C≡CAu was not observed. ^{31}P{^{1}H} (162.3 MHz, DMSO-d_6): δ 42.6 (s). ESI-MS m/z: 1747 ($[Zn(TpylC_6H_4C{\equiv}CAuPPh_3)_2(ClO_4)]^+$, 823 ($[Zn(TpylC_6H_4C{\equiv}CAuPPh_3)_2]^{2+}$), 721 ($[Au(PPh_3)_2]^+$). Exact m/z calcd. for ($[Zn(TpylC_6H_4C{\equiv}CAuPPh_3)_2]^{2+}$): 823.1405; found: 823.1407; Δ = 0.2 ppm.

$[Co(TpylC_6H_4C{\equiv}CAuPPh_3)_2](BF_4)_2$. Prepared from $TpylC_6H_4C{\equiv}CAuPPh_3$ (104 mg, 0.13 mmol) and $Co(BF_4)_2{\cdot}6H_2O$ (22 mg, 0.065 mmol). An orange solid was obtained. Yield: 106 mg, 0.057 mmol, 88%. Mp: 240 °C (d). Anal. Calcd for $C_{82}H_{58}Au_2B_2CoF_8N_6P_2{\cdot}(H_2O)_3$: C 52.67, H 3.45, N 4.49. Found: C 52.90, H 3.44, N 4.77. IR (KBr) $\tilde{\nu}$ (cm^{-1}): 2099 (C≡C), 1057 (B−F). ^{1}H NMR (400.9 MHz, CD_3CN): δ 91.65 (br s, 4H, H6), 53.56 (s, 4H, H3), 40.84 (s, 4H, H3′), 32.32 (s, 4H, H5), 13.67 (vd, J = 4.2 Hz, 4H, C_6H_4), 9.51 (s, 4H, H4), 9.05 (vd, J = 4.2 Hz, 4H, C_6H_4), 7.90−7.81 (m, 30H, Ph). ^{13}C{^{1}H} NMR (75.5 MHz, CD_3CN): δ 153.3 (C4), 142.1 (CH, C_6H_4), 135.4 (d, $^2J_{PC}$ = 12.5 Hz, *o*-Ph), 133.2 (s, *p*-Ph), 130.7 (d, $^3J_{PC}$ = 9.1 Hz, *m*-Ph), 121.2 (CH, C_6H_4). Owing to the paramagnetic effect, most of the signals of the $TpylC_6H_4C{\equiv}C$ unit were not observed.

$^{31}P\{^{1}H\}$ NMR (162.29 MHz, CD_3CN): δ 44.4 (s). ^{19}F NMR (282.4 MHz, CD_3CN): δ −150.29 (br s, $^{10}BF_4^-$), −150.34 (br s, $^{11}BF_4^-$). ESI-MS *m*/*z*: 1124 ($[Co_2(TpylC_6H_4C{\equiv}CAuPPh_3)_4(BF_4)]^{3+}$), 821 ($[Co(TpylC_6H_4C{\equiv}CAuPPh_3)_2]^{2+}$), 722, 592 [$(PPh_3PAuC{\equiv}C$-$C_6H_4Tpyl)Co(TpylC_6H_4C{\equiv}CH)_2]^{2+}$). Exact *m*/*z* calcd. for ($[Co(TpylC_6H_4C{\equiv}CAuPPh_3)_2]^{2+}$): 820.6425; found: 820.6447; Δ = 2.7 ppm.

$[Fe(TpylC_6H_4C{\equiv}CAuCNXy)_2](ClO_4)_2$. Prepared from $TpylC_6H_4$-$C{\equiv}CAuCNXy$ (71 mg, 0.11 mmol) and $Fe(ClO_4)_2{\cdot}6.4H_2O$ (20 mg, 0.054 mmol). A purple solid was obtained. Yield: 83 mg, 0.053 mmol, 97%. Mp: 303−308 °C (d). Anal. Calcd for $C_{64}H_{46}Au_2Cl_2FeN_8O_8$: C 48.78, H 2.94, N 7.11. Found: C 48.58, H 2.99, N 7.15. IR (KBr) $\tilde{\nu}$ (cm^{-1}): 2198 (C≡N), 2116 (C≡C). ^1H NMR (600.1 MHz, DMSO-d_6): δ 9.68 (s, 4H, H3′), 9.07 (d, $^3J_{HH}$ = 7.9 Hz, 4H, H3), 8.54 (vd, *J* = 8.5 Hz 4H, H6′), 8.04 (t, $^3J_{HH}$ = 7.7 Hz, 4H, H4), 7.75 (vd, *J* = 7.9 Hz 4H, H7′), 7.49 (t, $^3J_{HH}$ = 7.6 Hz, 2H, Xy), 7.36 (d, $^3J_{HH}$ = 7.6 Hz, 4H, Xy), 7.28 (d, $^3J_{HH}$ = 5.5 Hz, 4H, H6), 7.18 (t, $^3J_{HH}$ = 6.4 Hz, 4H, H5), 2.48 (s, 12H, Me, Xy). $^{13}C\{^1H\}$ NMR (75.5 MHz, DMSO-d_6): δ 159.9 (C2′), 157.9 (C2), 152.8 (C6), 148.1 (C8′), 138.7 (C4), 136.2 (C2, Xy), 134.1 (C5′), 132.5 (C7′), 131.3 (C4, Xy), 129.0 (AuC≡C), 128.4 (C3, Xy), 127.7 (C6′), 127.6 (C5), 127.1 (C4′), 124.1 (C3), 123.7 (br s, C1, Xy), 120.7 (C3′), 102.9 (C≡CAu), 18.1 (s, Me, Xy). The signal of the AuC≡N was not observed. ESI-MS *m*/*z*: 1421 ($[Fe(HCO_2)(TpylC_6H_4C{\equiv}CAuCNXy)_2]^+$), 761 ($[Fe(HCO_2)(TpylC_6H_4C{\equiv}CAuCNXy)]^+$), 688 ($[Fe(TpylC_6H_4C{\equiv}CAuCNXy)_2]^{2+}$), 636 ($[(XyNCAuC{\equiv}CC_6H_4Tpyl)Fe(TpylC_6H_4C{\equiv}CAuCO)]^{2+}$), 524.

$[Zn(TpylC_6H_4C{\equiv}CAuCNXy)_2](TfO)_2$. Prepared from $Zn(TfO)_2$ (18 mg, 0.050 mmol) and $TpylC_6H_4C{\equiv}CAuCNXy$ (67 mg, 0.10 mmol). A light yellow solid was obtained. Yield: 80 mg, 0.047 mmol, 94%. Mp: 220 °C (d). Anal. Calcd for $C_{66}H_{46}Au_2F_6N_8O_6S_2Zn{\cdot}(H_2O)_{1.5}$: C 46.31, H 2.89, N 6.55, S 3.75. Found: C 46.32, H 2.77, N 6.62, S 3.78. IR (KBr) $\tilde{\nu}$ (cm^{-1}): 2197 (C≡N), 2122 (C≡C), 1260 (SO), 1031 (CF), 638 (SO_2). ^1H NMR (400.9 MHz, DMSO-d_6): δ 9.39 (s, 4H, H3′), 9.16 (d, $^3J_{HH}$ = 8.0 Hz, 4H, H3), 8.42 (vd, *J* = 7.6 Hz, 4H, H6′), 8.29 (t, $^3J_{HH}$ = 7.6 Hz, 4H, H4), 7.95 (d, $^3J_{HH}$ = 4.4 Hz, 4H, H6), 7.69 (vd, *J* = 7.6 Hz, 4H, H7′), 7.51−7.46 (m, 6H, H5 and H4′, Xy), 7.35 (d, $^3J_{HH}$ = 7.6 Hz, 4H, H3, Xy), 2.47 (s, 12H, Me). $^{13}C\{^1H\}$ NMR (100.8 MHz, DMSO-d_6): δ 154.2 (C8′ or C4′), 149.5 (C2′), 147.8 (C6), 147.7 (C2), 141.3 (C4), 136.2 (C2, Xy), 133.6 (C5′), 132.5 (C7′), 131.2 (C5), 129.4 (C4′ or C8′), 128.5 (C3, Xy), 128.2 (C6′), 127.7 (C4, Xy), 123.6 (C3), 120.7 (C3′), 120.6 (q, $^1J_{FC}$ = 320.3 Hz, CF_3), 102.7 (s, C≡CAu), 18.1 (s, Me). The C−Au−C≡N−C signals were not observed. ^{19}F NMR (282.4 MHz, DMSO-d_6): δ −76.5 (s). ESI-MS *m*/*z*: 1429 ($[Zn(HCO_2)(TpylC_6H_4C{\equiv}CAuCNXy)_2]^+$), 769 ($[Zn(HCO_2)(TpylC_6H_4C{\equiv}CAuCNXy)]^+$), 692 ($[Zn(TpylC_6H_4C{\equiv}CAuCNXy)_2]^{2+}$), 661 ($[H(TpylC_6H_4C{\equiv}C)Au(CNXy)]^+$), 641 ($[(XyNCAuC{\equiv}CC_6H_4Tpyl)Zn(TpylC_6H_4C{\equiv}CAuCO)]^{2+}$), 589 ($[Zn(TpylC_6H_4C{\equiv}CAuCO)_2]^{2+}$), 310 ($[Zn(TpylC_6H_4C{\equiv}CAuCO)]^{2+}$).

$[Co(TpylC_6H_4C{\equiv}CAuCNXy)_2](BF_4)_2$. Prepared from $Co(BF_4)_2{\cdot}6H_2O$ (14 mg, 0.041 mmol) and $TpylC_6H_4C{\equiv}CAuCNXy$ (55 mg, 0.083 mmol). An orange solid was obtained. Yield: 60 mg, 0.038 mmol, 93%. Mp: 250 °C (d). Anal. Calcd for $C_{64}H_{46}Au_2B_2CoF_8N_8{\cdot}(H_2O)_2$: C 48.36, H 3.17, N 7.05. Found: C 48.46, H 3.02, N 6.95. IR (KBr) $\tilde{\nu}$ (cm^{-1}): 2200 (C≡N), 2116 (C≡C), 1056 (B−F). ^1H NMR (400.9 MHz, CD_3CN): δ 91.94 (br s, 4H, H6), 53.67 (s, 4H, H3), 40.95 (s, 4H, H3′), 32.48 (s, 4H, H5), 13.75 (s, 4H, C_6H_4), 9.60 (s, 4H, H4), 9.12 (s, 4H, C_6H_4), 7.68 (t, $^3J_{HH}$ = 7.6 Hz, 2H, Xy), 7.56 (d, $^3J_{HH}$ = 7.6 Hz, 4H, Xy), 2.84 (s, 12H, Me, Xy). $^{13}C\{^1H\}$ NMR (100.8 MHz, CD_3CN): δ 160.9, 159.6, 153.5 (C4), 142.4 (CH, C_6H_4), 137.8 (C2, Xy), 132.5 (C4, Xy), 129.7 (C3, Xy), 127.5, 125.4, 121.1 (CH, C_6H_4), 109.1 (C≡CAu), 19.2 (s, Me). Owing to the paramagnetic effect, 8 of the expected 20 signals were not observed. ^{19}F NMR (282.4 MHz, CD_3CN): δ −150.19 (br s, $^{10}BF_4^-$), −150.24 (br s, $^{11}BF_4^-$). ESI-MS *m*/*z*: 690 ($[Co(TpylC_6H_4C{\equiv}CAuCNXy)_2]^{2+}$), 590, 325, 235, 222. Exact *m*/*z* calcd. for ($[Co(TpylC_6H_4C{\equiv}CAuCNXy)_2]^{2+}$): 689.6249; found: 689,6250; Δ = 0.15 ppm.

Synthesis of $[M\{(TpylC_6H_4C{\equiv}C)_2Au\}]_nX_n$ (M = Fe, Co, Zn; X = ClO_4, BF_4). To a solution of $PPN[(TpylC_6H_4C{\equiv}C)_2Au]$ in CH_2Cl_2 (3 mL), a solution of $MX_2{\cdot}nH_2O$ in MeCN (10 mL) was added. Immediately, a suspension was formed, which was stirred at room temperature for 30 min. The suspension was filtered and the isolated solid was washed with CH_2Cl_2 (2 × 5 mL), acetone (2 × 5 mL), and Et_2O (3 × 5 mL), and dried under a vacuum.

$[Fe\{(TpylC_6H_4C{\equiv}C)_2Au\}]_n(ClO_4)_n$. Prepared from $Fe(ClO_4)_2{\cdot}6.4H_2O$ (18 mg, 0.050 mmol) and $PPN[(TpylC_6H_4C{\equiv}C)_2Au]$ (70 mg, 0.050 mmol). Purple solid. Yield: 47 mg, 0.046 mmol, 92%. Mp: > 310 °C. Anal. Calcd for $(C_{46}H_{28}AuFeN_6ClO_4)_{4.3}{\cdot}Fe(ClO_4)_2{\cdot}(H_2O)_{9.9}$: C, 49.43; H, 2.94; N, 7.52. Found: C 49.46, H 2.94, N 7.53. IR (KBr) $\tilde{\nu}$ (cm^{-1}): 2087 (C≡C), 1080, 619 (ClO_4^-). ^1H NMR (300.1 MHz, DMSO-d_6): δ 9.66 (s, 4H, H3′), 9.07 (d, $^3J_{HH}$ = 7.7 Hz, 4H, H3), 8.47 (vd, *J* = 7.5 Hz, 4H, H6′), 8.02 (t, $^3J_{HH}$ = 7.1 Hz, 4H, H4), 7.63 (vd, *J* = 7.5 Hz, 4H, H7′), 7.27 (d, $^3J_{HH}$ = 3.8 Hz, 4H, H6), 7.17 (t, $^3J_{HH}$ = 6.8 Hz, 4H, H5). Owing to the low solubility of this compound, we could not obtain an useful $^{13}C\{^1H\}$ NMR spectrum. ESI-MS (R^{tpy} = $TpylC_6H_4C{\equiv}C$) *m*/*z*: 984 ($[Fe_5R^{tpy}{}_{11}Au_5H]^{5+}$), 779 ($[Fe_7R^{tpy}{}_{14}Au_6H_2]^{8+}$), 771 ($[Fe_3R^{tpy}{}_7Au_3H]^{4+}$), 759 ($[Fe_6R^{tpy}{}_{12}Au_5H_2]^{7+}$), 732 ($[Fe_5R^{tpy}{}_{10}Au_4H_2]^{6+}$), 723 ($[Fe_2R^{tpy}{}_5Au_2H]^{3+}$), 699 (*z* = 3), 695 ($[Fe_4R^{tpy}{}_8Au_3H_2]^{5+}$), 639 ($[Fe_3R^{tpy}{}_6Au_2H_2]^{4+}$), 590 (*z* = 2), 547 ($[Fe_2R^{tpy}{}_4AuH_2]^{3+}$), 473 ($[FeR^{tpy}{}_2AuH(CO)]^{2+}$), 361 ($[Fe(R^{tpy}H)_2]^{2+}$).

$[Zn\{(TpylC_6H_4C{\equiv}C)_2Au\}]_n(ClO_4)_n$. Prepared from $PPN[(TpylC_6H_4C{\equiv}C)_2Au]$ (57 mg, 0.041 mmol) and $Zn(ClO_4)_2{\cdot}6H_2O$ (15 mg, 0.041 mmol). Yellow solid. Yield: 40 mg, 0.039 mmol; 96%. Mp: > 300 °C. Anal. Calcd for $(C_{46}H_{28}AuClN_6O_4Zn)_{4.3}{\cdot}[Zn(ClO_4)_2]{\cdot}(H_2O)_{6.4}$: C, 49.56; H, 2.80; N, 7.54. Found: C, 49.54; H, 2.80; N, 7.52. IR (KBr) $\tilde{\nu}$ (cm^{-1}): 2090 (C≡C), 1080, 621 (ClO_4^-). ^1H NMR (400.9 MHz, DMSO-d_6): δ 9.40 (br s, 4H, H3′), 9.18 (br s, 4H, H3), 8.38−8.30 (br m, 8H, H6′ and H4), 7.97 (br s, 4H, H6), 7.52 (br m, 8H, H5 and H7′). $^{13}C\{^1H\}$ NMR (100.8 MHz, DMSO-d_6): δ 149.4, 147.7, 141.3, 132.0, 128.0, 127.6, 120.4 (all signals are broad and correspond to the CH's of the C_6H_4Tpyl group). ESI-MS (R^{tpy} = $TpylC_6H_4C{\equiv}C$, MeCN) *m*/*z*: 2514 (*z* = 1), 2482 (*z* = 1), 2281 ($[ZnR^{tpy}{}_4Au_4(ClO_4)]^+$), 2217 ($[ZnR^{tpy}{}_4Au_4Cl]^+$), 1985 ($[ZnR^{tpy}{}_4Au_3]^+$), 1953 ($[Zn_2R^{tpy}{}_4Au_2(ClO_4)]^+$), 1784 ($[Au_4R^{tpy}{}_3]^+$), 1752 ($[ZnR^{tpy}{}_3Au_3(ClO_4)]^+$), 1688 ($[ZnR^{tpy}{}_3Au_3Cl]^+$), 1454 ($[ZnR^{tpy}{}_3Au_2]^+$) 1307 ($[Zn_3R^{tpy}{}_5Au_3Cl_2(H_2O)(Me_2SO)]^{2+}$), 1255 ($Au_3R^{tpy}{}_2]^+$), 1191 ($[Zn_2R^{tpy}{}_5Au_3]^{2+}$), 1128 (*z* = 1), 963 (*z* = 1), 925 ($[ZnR^{tpy}{}_2Au]^+$) 656 ($[ZnR^{tpy}Au(HCO_2)(H_2O)]^+$). ESI-MS (MeOH) *m*/*z*: 1059 ($[Zn_4R^{tpy}{}_9Au_5]^{4+}$), 629 (*z* = 1), 463 (*z* = 1), 413 (*z* = 1).

$[Co\{(TpylC_6H_4C{\equiv}C)_2Au\}]_n(BF_4)_n$. Prepared from $PPN[(TpylC_6H_4C{\equiv}C)_2Au]$ (63 mg, 0.045 mmol) and $Co(BF_4)_2{\cdot}6H_2O$ (15 mg, 0.044 mmol). Orange brown solid. Yield: 42 mg, 0.041 mmol, 92%. Mp: > 300 °C. Anal. Calcd for $(C_{46}H_{28}AuBCoF_4N_6)_{8.8}{\cdot}[Co(BF_4)_2]{\cdot}(H_2O)_{4.8}$: C, 52.94; H, 2.81; N, 8.05. Found: C, 52.92; H, 2.81; N, 7.85. IR (KBr) $\tilde{\nu}$ (cm^{-1}): 2095 (C≡C), 1056 (B−F). ^1H NMR (400.9 MHz, DMSO-d_6): δ 83.50 (br s, 4H, H6), 48.79 (br s, 4H, H3), 32.39 (br s, 4H, H3′), 30.45 (br s, 4H, H5), 13.51 (br s, 4H, C_6H_4), 10.49 (br s, 4H, H4), 8.71 (br s, 4H, C_6H_4). Owing to the low solubility of this compound, we could not obtain an useful $^{13}C\{^1H\}$ NMR spectrum. ^{19}F NMR (282.4 MHz, DMSO-d_6): δ −147.68 (br s, $^{10}BF_4^-$), −147.74 (br s, $^{11}BF_4^-$). ESI-MS *m*/*z*: 1449 ($[Co(TpylC_6H_4C{\equiv}C)_3Au_2]^+$), 1185 ($[Co_2(TpylC_6H_4C{\equiv}C)_5Au_3]^{2+}$), 998 ($[Co_2\{(TpylC_6H_4C{\equiv}C)_2Au\}(Me_2SO)_2]^{2+}$), 920 ($[Co_2\{(TpylC_6H_4C{\equiv}C)_2Au\}]^{2+}$), 644, 538, 470, 420.

X-ray Crystallography. Crystals of $[Fe(TpylC_6H_4C{\equiv}CAuCNXy)_2](ClO_4)_2{\cdot}(MeCN)_2$ and $[Co(TpylC_6H_4C{\equiv}CAuPPh_3)_2](BF_4)_2{\cdot}(MeCN)_4$ were obtained by liquid diffusion between a MeCN solution and toluene, and were measured on Bruker Smart APEX and D8 QUEST diffractometers, respectively. Data were collected using monochromated Mo−Kα radiation in ω-scan mode. The structures were solved by direct methods and refined anisotropically on F^2 using the programs SHELXL-2013 and -2014, respectively (G. M. Sheldrick, University of Göttingen).[97] *Special features of refinement:* For complex $[Co(TpylC_6H_4C{\equiv}CAuPPh_3)_2](BF_4)_2$ one of the BF_4 anions is disordered over two positions, ca. 63:37%. One of the acetonitrile molecules is disordered over two positions, ca. 54:46%. In $[Fe(TpylC_6H_4C{\equiv}CAuCNXy)_2](ClO_4)_2$ both perchlorate anions are disordered over two positions, one Xy group is either disordered over two positions, and one of the crystallization acetonitrile molecules is disordered over two positions. Relevant crystal data and details about data acquisition and structure refinement are given in Table 2. CIF files containing full crystallographic details are included in the Supporting Information and have been also deposited in the Cambridge Crystallographic Data Centre (CCDC 1043100 (Fe complex) and 1043099 (Co complex)). These data can be obtained free of charge via www.ccdc.cam.ac.uk/data_request/cif.

■ ASSOCIATED CONTENT

Supporting Information

Crystallographic information in CIF format, NMR spectra, and additional crystal structure data. The Supporting Information is available free of charge on the ACS Publications website at DOI: 10.1021/acs.inorgchem.5b00176.

■ AUTHOR INFORMATION

Corresponding Authors

*(J.G.-R.) E-mail: jgr@um.es. Webpage: http://www.um.es/gqo/

*(J.V.) E-mail: jvs1@um.es. Webpage: http://www.um.es/gqo/.

Notes

The authors declare no competing financial interest.

■ ACKNOWLEDGMENTS

We thank the Spanish Ministerio de Economía y Competitividad (Grant CTQ2011-24016, with FEDER support) and Fundación Séneca (Grant 04539/GERM/06) for financial support. We also thank Dr. J. G. Hernández Cifre and Ms. V. Fernández Espín for carrying out DLS measurements.

■ REFERENCES

(1) Constable, E. C. *Chem. Soc. Rev.* **2007**, *36*, 246.

(2) Schubert, U. S.; Eschbaumer, C. *Angew. Chem., Int. Ed.* **2002**, *41*, 2892.

(3) Wild, A.; Winter, A.; Schlutter, F.; Schubert, U. S. *Chem. Soc. Rev.* **2011**, *40*, 1459.

(4) Hofmeier, H.; Schubert, U. S. *Chem. Soc. Rev.* **2004**, *33*, 373.

(5) Yan, Y.; Huang, J. *Coord. Chem. Rev.* **2010**, *254*, 1072.

(6) Holyer, R. H.; Hubbard, C. D.; Kettle, S. F. A.; Wilkins, R. G. *Inorg. Chem.* **1966**, *5*, 622.

(7) Dobrawa, R.; Würthner, F. *J. Polym. Sci., Part A: Polym. Chem.* **2005**, *43*, 4981.

(8) Hogg, R.; Wilkins, R. G. *J. Chem. Soc.* **1962**, 341.

(9) Hayami, S.; Moriyama, R.; Shigeyoshi, Y.; Kawajiri, R.; Mitani, T.; Akita, M.; Inoue, K.; Maeda, Y. *Inorg. Chem.* **2005**, *44*, 7295.

(10) Barigelletti, F.; Flamigni, L. *Chem. Soc. Rev.* **2000**, *29*, 1.

(11) Ziessel, R.; Hissler, M.; El-ghayoury, A.; Harriman, A. *Coord. Chem. Rev.* **1998**, *178−180*, 1251.

(12) Harriman, A.; Ziessel, R. *Chem. Commun.* **1996**, 1707.

(13) Barboiu, M.; Vaughan, G.; Graff, R.; Lehn, J.-M. *J. Am. Chem. Soc.* **2003**, *125*, 10257.

(14) Flamigni, L.; Collin, J.-P.; Sauvage, J.-P. *Acc. Chem. Res.* **2008**, *41*, 857.

(15) Constable, E. C.; Harris, K.; Housecroft, C. E.; Neuburger, M. *Dalton Trans.* **2011**, *40*, 1524.

(16) Wang, J.-L.; Li, X.; Lu, X.; Hsieh, I. F.; Cao, Y.; Moorefield, C. N.; Wesdemiotis, C.; Cheng, S. Z. D.; Newkome, G. R. *J. Am. Chem. Soc.* **2011**, *133*, 11450.

(17) Chan, Y.-T.; Li, X.; Yu, J.; Carri, G. A.; Moorefield, C. N.; Newkome, G. R.; Wesdemiotis, C. *J. Am. Chem. Soc.* **2011**, *133*, 11967.

(18) Wang, M.; Wang, C.; Hao, X.-Q.; Li, X.; Vaughn, T. J.; Zhang, Y.-Y.; Yu, Y.; Li, Z.-Y.; Song, M.-P.; Yang, H.-B.; Li, X. *J. Am. Chem. Soc.* **2014**, *136*, 10499.

(19) Xie, T.-Z.; Liao, S.-Y.; Guo, K.; Lu, X.; Dong, X.; Huang, M.; Moorefield, C. N.; Cheng, S. Z. D.; Liu, X.; Wesdemiotis, C.; Newkome, G. R. *J. Am. Chem. Soc.* **2014**, *136*, 8165.

(20) Puntoriero, F.; Campagna, S.; Stadler, A.-M.; Lehn, J.-M. *Coord. Chem. Rev.* **2008**, *252*, 2480.

(21) Osawa, M.; Hoshino, M.; Horiuchi, S.; Wakatsuki, Y. *Organometallics* **1998**, *18*, 112.

(22) Gohy, J.-F.; Chiper, M.; Guillet, P.; Fustin, C.-A.; Hoeppener, S.; Winter, A.; Hoogenboom, R.; Schubert, U. S. *Soft Matter* **2009**, *5*, 2954.

(23) Wang, J.-L.; Chan, Y.-T.; Moorefield, C. N.; Pei, J.; Modarelli, D. A.; Romano, N. C.; Newkome, G. R. *Macromol. Rapid Commun.* **2010**, *31*, 850.

(24) Fermi, A.; Bergamini, G.; Roy, M.; Gingras, M.; Ceroni, P. *J. Am. Chem. Soc.* **2014**, *136*, 6395.

(25) Constable, E. C.; Thompson, A. M. W. C. *J. Chem. Soc., Dalton Trans.* **1992**, 3467.

(26) Kurth, D. G.; Higuchi, M. *Soft Matter* **2006**, *2*, 915.

(27) Friese, V. A.; Kurth, D. G. *Coord. Chem. Rev.* **2008**, *252*, 199.

(28) Winter, A.; Friebe, C.; Chiper, M.; Hager, M. D.; Schubert, U. S. *J. Polym. Sci., Part A: Polym. Chem.* **2009**, *47*, 4083.

(29) He, L.; Liang, J.; Cong, Y.; Chen, X.; Bu, W. *Chem. Commun.* **2014**, *50*, 10841.

(30) Stepanenko, V.; Stocker, M.; Muller, P.; Buchner, M.; Würthner, F. *J. Mater. Chem.* **2009**, *19*, 6816.

(31) Han, F. S.; Higuchi, M.; Kurth, D. G. *J. Am. Chem. Soc.* **2008**, *130*, 2073.

(32) Han, F. S.; Higuchi, M.; Kurth, D. G. *Adv. Mater.* **2007**, *19*, 3928.

(33) Burnworth, M.; Mendez, J. D.; Schroeter, M.; Rowan, S. J.; Weder, C. *Macromolecules* **2008**, *41*, 2157.

(34) Chen, Y.-Y.; Tao, Y.-T.; Lin, H.-C. *Macromolecules* **2006**, *39*, 8559.

(35) Kelch, S.; Rehahn, M. *Macromolecules* **1999**, *32*, 5818.

(36) El-Ghayoury, A.; Schenning, A. P. H. J.; Meijer, E. W. *J. Polym. Sci., Part A: Polym. Chem.* **2002**, *40*, 4020.

(37) Storrier, G. D.; Colbran, S. B.; Craig, D. C. *J. Chem. Soc., Dalton Trans.* **1997**, 3011.

(38) Dobrawa, R.; Lysetska, M.; Ballester, P.; Grüne, M.; Würthner, F. *Macromolecules* **2005**, *38*, 1315.

(39) Groger, G.; Stepanenko, V.; Würthner, F.; Schmuck, C. *Chem. Commun.* **2009**, 698.

(40) Iyer, P. K.; Beck, J. B.; Weder, C.; Rowan, S. J. *Chem. Commun.* **2005**, 319.

(41) Schwarz, G.; Bodenthin, Y.; Geue, T.; Koetz, J.; Kurth, D. G. *Macromolecules* **2010**, *43*, 494.

(42) Yu, S. C.; Kwok, C. C.; Chan, W. K.; Che, C. M. *Adv. Mater.* **2003**, *15*, 1643.

(43) Han, F. S.; Higuchi, M.; Ikeda, T.; Negishi, Y.; Tsukuda, T.; Kurth, D. G. *J. Mater. Chem.* **2008**, *18*, 4555.

(44) Ng, W. Y.; Gong, X.; Chan, W. K. *Chem. Mater.* **1999**, *11*, 1165.

(45) Kimura, M.; Horai, T.; Muto, T.; Hanabusa, K.; Shirai, H. *Chem. Lett.* **1999**, *28*, 1129.

(46) Lima, J. C.; Rodríguez, L. *Chem. Soc. Rev.* **2011**, *40*, 5442.

(47) Schmidbaur, H.; Schier, A. *Chem. Soc. Rev.* **2012**, *41*, 370.

(48) Schmidbaur, H.; Schier, A. *Chem. Soc. Rev.* **2008**, *37*, 1931.

(49) Yam, V. W.-W.; Cheng, E. C.-C. *Chem. Soc. Rev.* **2008**, *37*, 1806.

(50) Lu, W.; Kwok, W.-M.; Ma, C.; Chan, C. T.-L.; Zhu, M.-X.; Che, C.-M. *J. Am. Chem. Soc.* **2011**, *133*, 14120.

(51) Tong, G. S. M.; Chow, P. K.; Che, C.-M. *Angew. Chem., Int. Ed.* **2010**, *49*, 9206.

(52) Rodríguez, L.; Ferrer, M.; Crehuet, R.; Anglada, J.; Lima, J. C. *Inorg. Chem.* **2012**, *51*, 7636.

(53) Puddephatt, R. J. *Coord. Chem. Rev.* **2001**, *216−217*, 313.

(54) Puddephatt, R. J. *Chem. Soc. Rev.* **2008**, *37*, 2012.

(55) Langdon-Jones, E. E.; Pope, S. J. A. *Chem. Commun.* **2014**, *50*, 10343.

(56) Meng, X.; Moriuchi, T.; Kawahata, M.; Yamaguchi, K.; Hirao, T. *Chem. Commun.* **2011**, *47*, 4682.

(57) Panciera, M.; Amorín, M.; Castedo, L.; Granja, J. R. *Chem.—Eur. J.* **2013**, *19*, 4826.

(58) Hong, E. Y.-H.; Wong, H.-L.; Yam, V. W.-W. *Chem. Commun.* **2014**, *50*, 13272.

(59) Gavara, R.; Llorca, J.; Lima, J. C.; Rodríguez, L. *Chem. Commun.* **2013**, *49*, 72.

(60) Cámara, V.; Masciocchi, N.; Gil-Rubio, J.; Vicente, J. *Chem.—Eur. J.* **2014**, *20*, 1389.

(61) Vicente, J.; Gil-Rubio, J.; Barquero, N.; Cámara, V.; Masciocchi, N. *Chem. Commun.* **2010**, *46*, 1053.

(62) Cámara, V.; Barquero, N.; Bautista, D.; Gil-Rubio, J.; Vicente, J. *Chem.—Eur. J.* **2015**, *21*, 1992.

(63) Vicente, J.; Gil-Rubio, J.; Barquero, N.; Jones, P. G.; Bautista, D. *Organometallics* **2008**, *27*, 646.

(64) Constable, E. C.; Housecroft, C. E.; Neuburger, M.; Schaffner, S.; Shardlow, E. J. *Dalton Trans.* **2007**, 2631.

(65) Constable, E. C.; Housecroft, C. E.; Kocik, M. K.; Zampese, J. A. *Polyhedron* **2011**, *30*, 2704.

(66) Li, X.-L.; Zhang, K.-J.; Li, J.-J.; Cheng, X.-X.; Chen, Z.-N. *Eur. J. Inorg. Chem.* **2010**, 3449.

(67) Chow, H. S.; Constable, E. C.; Housecroft, C. E.; Kulicke, K. J.; Tao, Y. *Dalton Trans.* **2005**, 236.

(68) Constable, E. C.; Harris, K.; Housecroft, C. E.; Neuburger, M.; Zampese, J. A. *CrystEngComm* **2010**, *12*, 2949.

(69) Elsbernd, H.; Beattie, J. K. *J. Inorg. Nucl. Chem.* **1972**, *34*, 771.

(70) Padhi, S. K.; Sahu, R.; Saha, D.; Manivannan, V. *Inorg. Chim. Acta* **2011**, *372*, 383.

(71) Pitarch López, J.; Kraus, W.; Reck, G.; Thünemann, A.; Kurth, D. G. *Inorg. Chim. Acta* **2005**, *358*, 3384.

(72) Beves, J. E.; Chwalisz, P.; Constable, E. C.; Housecroft, C. E.; Neuburger, M.; Schaffner, S.; Zampese, J. A. *Inorg. Chem. Commun.* **2008**, *11*, 1009.

(73) Hayami, S.; Komatsu, Y.; Shimizu, T.; Kamihata, H.; Lee, Y. H. *Coord. Chem. Rev.* **2011**, *255*, 1981.

(74) Galet, A.; Gaspar, A. B.; Muñoz, M. C.; Real, J. A. *Inorg. Chem.* **2006**, *45*, 4413.

(75) Irwin, M. J.; Jia, G.; Payne, N. C.; Puddephatt, R. J. *Organometallics* **1996**, *15*, 51.

(76) Xiao, H.; Cheung, K.-K.; Che, C.-M. *J. Chem. Soc., Dalton Trans.* **1996**, 3699.

(77) Pastor, A.; Martínez-Viviente, E. *Coord. Chem. Rev.* **2008**, *252*, 2314.

(78) Cohen, Y.; Avram, L.; Frish, L. *Angew. Chem., Int. Ed.* **2005**, *44*, 520.

(79) García de la Torre, J.; Bloomfield, V. A. *Q. Rev. Biophys.* **1981**, *14*, 81.

(80) Tirado, M. M.; López Martínez, C.; García de la Torre, J. *J. Chem. Phys.* **1984**, *81*, 2047.

(81) García de la Torre, J.; López Martínez, M. C.; Tirado, M. M. *Biopolymers* **1984**, *23*, 611.

(82) Hamelin, B.; Jullien, L.; Derouet, C.; Hervé du Penhoat, C.; Berthault, P. *J. Am. Chem. Soc.* **1998**, *120*, 8438.

(83) Wong, A.; Ida, R.; Spindler, L.; Wu, G. *J. Am. Chem. Soc.* **2005**, *127*, 6990.

(84) Riis-Johannessen, T.; Bernardinelli, G.; Filinchuk, Y.; Clifford, S.; Favera, N. D.; Piguet, C. *Inorg. Chem.* **2009**, *48*, 5512.

(85) Shestakova, P.; Absillis, G.; Martín-Martínez, F. J.; De Proft, F.; Willem, R.; Parac-Vogt, T. N. *Chem.—Eur. J.* **2014**, *20*, 5258.

(86) Maity, B.; Gadadhar, S.; Goswami, T. K.; Karande, A. A.; Chakravarty, A. R. *Dalton Trans.* **2011**, *40*, 11904.

(87) The length of the Fe monomeric unit was incremented in 0.4 Å to account for the increment in the Zn−N(axial) bond distance respect to the Fe−N(axial) bond distance in bis(terpyridine) complexes.

(88) Hassan, P. A.; Rana, S.; Verma, G. *Langmuir* **2015**, *31*, 3.

(89) de Hatten, X.; Asil, D.; Friend, R. H.; Nitschke, J. R. *J. Am. Chem. Soc.* **2012**, *134*, 19170.

(90) Du, G.; Moulin, E.; Jouault, N.; Buhler, E.; Giuseppone, N. *Angew. Chem., Int. Ed.* **2012**, *51*, 12504.

(91) Isla, H.; Pérez, E. M.; Martín, N. *Angew. Chem., Int. Ed.* **2014**, *53*, 5629.

(92) Jans, H.; Liu, X.; Austin, L.; Maes, G.; Huo, Q. *Anal. Chem.* **2009**, *81*, 9425.

(93) Hevekerl, H.; Wigenius, J.; Persson, G.; Inganäs, O.; Widengren, J. *J. Phys. Chem. B* **2014**, *118*, 5924.

(94) Grosshenny, V.; Romero, F. M.; Ziessel, R. *J. Org. Chem.* **1997**, *62*, 1491.

(95) Stoyanova, R.; Kuesel, A. C.; Brown, T. R. *J. Magn. Reson., Ser. A* **1995**, *115*, 265.

(96) Lide, D. R. *CRC Handbook of Chemistry and Physics*, Internet Version 2005; CRC Press: Boca Raton, FL, 2005.

(97) Sheldrick, G. M. *Acta Crystallogr.* **2008**, *A64*, 112.